

## The Therapeutic and Preventive Effect of RRR- $\alpha$ -Vitamin E Succinate on Prostate Cancer via Induction of Insulin-Like Growth Factor Binding Protein-3

Yi Yin,<sup>1,2</sup> Jing Ni,<sup>1</sup> Ming Chen,<sup>1</sup> Matthew A. DiMaggio,<sup>1</sup> Yinglu Guo,<sup>2</sup> and Shuyuan Yeh<sup>1</sup>

**Abstract Purpose:** Insulin-like growth factor binding protein-3 (IGFBP-3) is a well-known antiproliferative and proapoptotic molecule in prostate cancer, suggesting that targeting IGFBP-3 might produce clinical benefits. In prostate cancer cells, RRR- $\alpha$ -vitamin E succinate (VES) inhibits cell proliferation and induces apoptosis, yet the mechanisms remain to be elucidated. We hypothesize that the protective effects of VES in prostate cancer are mediated by IGFBP-3 up-regulation. Using prostate cancer models, the involvement of IGFBP-3 in the anticancer effect of VES was investigated.

**Experimental Design:** IGFBP-3 mRNA and protein were determined by real-time PCR and Western blotting in prostate cancer cells, xenografted tumors of nude mice, and prostate tumors of transgenic adenocarcinoma mouse prostate (TRAMP) mice. The serum levels of IGFBP-3 were assessed by ELISA. The importance of IGFBP-3 in VES-mediated antitumor effects was confirmed by small interfering RNA knockdown strategy.

**Results:** We found that VES induced IGFBP-3 mRNA and protein levels in human prostate cancer cell lines. Knockdown of IGFBP-3 by small interfering RNA attenuated VES-induced IGFBP-3 expression and VES-mediated antiproliferative and proapoptotic functions. Furthermore, administration of VES resulted in a significant therapeutic effect on LNCaP and PC3 xenografts and a preventive effect on tumorigenic progression in the TRAMP model without overt toxicity. Notably, the therapeutic and preventive efficacy of VES correlated with increased accumulation of IGFBP-3 in mouse serum as well as in the xenograft tumors and TRAMP prostate samples. Consequently, reduced proliferation and induced apoptosis were witnessed.

**Conclusions:** VES mediates its therapeutic and preventive effects against prostate cancer at least partially through up-regulating IGFBP-3, which inhibits cell proliferation and promotes cell apoptosis.

Prostate cancer is the third leading cause of male cancer death in the United States with an estimated 27,350 deaths in 2006 (1). Epidemiologic and preclinical observations suggest that  $\alpha$ -vitamin E derivatives provide protective effects for various malignant diseases (2). Accumulating evidences indicate that RRR- $\alpha$ -vitamin E succinate (VES), one of the most effective vitamin E analogues in terms of anticancer properties, inhibits growth of a wide variety of cancer cells and exhibits low toxicity in nonmalignant cells (3–5). Recent reports show that the antiprostate tumor effect of VES is via modulating the androgen receptor level (5), cell cycle machinery (6, 7), suppressing DNA

synthesis (8), inducing apoptosis (3), as well as inhibiting prostate cancer cell invasion (9). In addition, the absorption and function of VES in prostate cancer cells could be enhanced by the vitamin E binding proteins (10, 11). Despite a growing body of evidence that indicates VES as a promising agent against prostate cancer *in vitro*, the *in vivo* therapeutic or preventive efficacy and underlying mechanisms have not been fully elucidated.

In human, the serum level of insulin-like growth factor (IGF) binding protein-3 (IGFBP-3) has an inverse relationship with the risk of prostate cancer (12–16). Low-plasma IGFBP-3 levels have a predictive value in identifying individuals with advanced-stage prostate cancer (13). In animal models, IGFBP-3 is retentively low in the serum of the transgenic adenocarcinoma mouse prostate (TRAMP) model at its metastasis stage (17), indicating that IGFBP-3 might serve as a surrogate prognosis marker of aggressive prostate cancer (14). The classic mechanism of IGFBP-3, like other IGFBP family members, is to modulate the function of the IGF pathway (18). Recently, accumulating data suggest that IGFBP-3 has its own biological function via regulating the cell cycle, inducing apoptosis, and cross-talk with major signal transduction pathways (19). Results from transgenic mouse models indicate that inhibitory effects of IGFBP-3 on prostate cancer could be IGF dependent during the initiation of tumorigenesis and IGF independent as the cancer advances (20).

**Authors' Affiliations:** <sup>1</sup>Departments of Urology and Pathology, George Whipple Laboratory for Cancer Research, University of Rochester, Rochester, New York and <sup>2</sup>Peking University First Hospital, Institute of Urology of Peking University, Beijing, China

Received 5/30/06; revised 12/12/06; accepted 1/11/07.

**Grant support:** NIH grant DK60912.

The costs of publication of this article were defrayed in part by the payment of page charges. This article must therefore be hereby marked *advertisement* in accordance with 18 U.S.C. Section 1734 solely to indicate this fact.

**Requests for reprints:** Shuyuan Yeh, Departments of Urology and Pathology, University of Rochester, Rochester, NY 14642. Phone: 585-275-3346; Fax: 585-273-1068; E-mail: shuyuan\_yeh@urmc.rochester.edu.

© 2007 American Association for Cancer Research.

doi:10.1158/1078-0432.CCR-06-1217

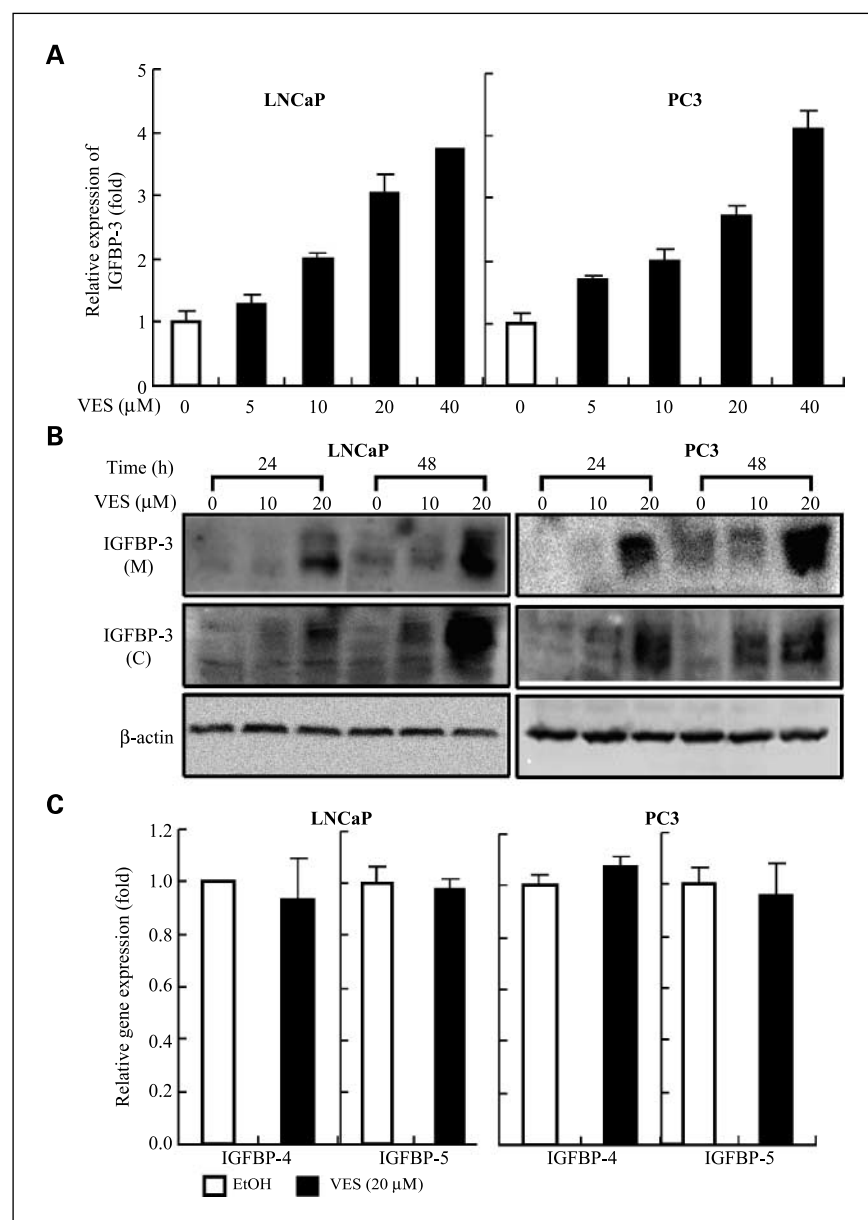


**Fig. 1.** VES dose dependently induces gene expression of IGFBP-3, but not IGFBP-4 and IGFBP-5, in human prostate cancer cells. **A**, IGFBP-3 mRNA expressions are induced by VES. Serum-starved LNCaP and PC3 cells were treated with either vehicle or VES at indicated doses in SFM for 24 h. RNA was reverse transcribed and quantitated by real-time PCR. **B**, secretory and cellular IGFBP-3 protein levels are increased by VES treatment. Prostate cancer cells were serum starved for 24 h and then treated with vehicle or VES (10 and 20 μmol/L) for 24 and 48 h. Cell lysates (**C**) and concentrated culture media (**M**) were prepared for IGFBP-3 Western blotting analysis. **C**, IGFBP-4 and IGFBP-5 mRNA expression levels are not affected by VES treatment in prostate cancer cells. The RNA samples harvested in (**A**) were analyzed by real-time PCR for the expression of IGFBP-4 and IGFBP-5. Columns, mean of triplicate experiments; bars, SD.

Accumulating evidences also suggest that VES provides protective effects against prostate cancer *in vitro* via regulating cell cycle effectors and inducing apoptosis (3, 5, 6, 9). However, little is known about whether VES has therapeutic or preventive effects for prostate cancer *in vivo* and whether VES might function through modulation of IGFBP-3. We hypothesize that the cancer protective effects of VES in prostate cancer are mediated by IGFBP-3 up-regulation. In the present study, we provide *in vitro* and *in vivo* evidences, which indicate that IGFBP-3 is involved in VES-mediated therapeutic and preventive effects on prostate cancer progression.

### Materials and Methods

**Cell culture.** The prostate cancer cell lines, LNCaP and PC3, were propagated at 37°C with 5% CO<sub>2</sub> in complete RPMI 1640 supplemented with 10% fetal bovine serum.

**Chemicals and reagents.** RRR-α-VES and cycloheximide were purchased from Sigma (St. Louis, MO). Antibodies for proliferating cell nuclear antigen (PCNA), SV40 T antigen (T-ag), and β-actin were obtained from Santa Cruz Biotechnology (Santa Cruz, CA). IGFBP-3 antibody was obtained from Diagnostic Systems Laboratories (Webster, TX). For the *in vitro* experiments, VES was dissolved in ethanol. For the *in vivo* experiments, we used DMSO as solvent to prevent irritation. The relative solvents were used as control in the individual experiment.

**Animal experiments.** Each flank of 6-week-old male athymic mice (Charles River, Wilmington, MA) was inoculated s.c. with 1 × 10<sup>6</sup> LNCaP cells in 0.1 mL of 100% Matrigel or 7.5 × 10<sup>5</sup> PC3 cells in 0.1 mL serum-free medium (SFM) containing 50% Matrigel (BD Biosciences, Bedford, MA). Once tumors became palpable (>50 mm<sup>3</sup>), mice were randomly divided into groups with seven mice per group and injected i.p. with vehicle or VES (100 mg/kg) twice weekly for 5 to 6 weeks. Body weights and xenograft sizes were measured as described previously (10).

Male heterozygous TRAMP mice in a pure C57BL/6 background were purchased from JAX Mice and Services (Bar Harbor, ME) and bred at the University of Rochester Medical Center in accordance with the

guidelines established by the University's Animal Research Committee. Transgene incorporation screening assays were done as described previously (21). Male TRAMP mice and nontransgenic littermates (5-6 weeks old) were randomly distributed into three groups ( $n = 12$ ) for prevention experiments and two groups ( $n = 10$ ) for VES toxicity experiments. Mice were injected i.p. with VES (50 or 100 mg/kg) or vehicle twice weekly until 32 weeks old. Male TRAMP mice (5-6 weeks old) were also injected i.p. twice weekly with VES (100 mg/kg) and vehicle for 8 weeks; the prostates were collected for SV40 large T-agg detection.

At necropsy, serum was collected and stored at  $-80^{\circ}\text{C}$ . For nude mice, tumor weights were measured. The xenograft tissues and several mouse organs (brain, heart, lungs, liver, kidneys, spleen, spinal cord, gastrointestinal, and genitourinary tract) were collected for H&E staining or stored in liquid nitrogen for further analysis. For TRAMP mice, the genitourinary apparatus consisting of bladder, urethra, seminal vesicles, ampullary gland, and the prostate was excised and weighed. The dorsolateral prostate was excised for histology analysis.

**Metastases examination.** The Indian ink staining was used to examine cancer metastasis to lungs as described previously (22). The metastasis to lymph nodes was observed under the microscope. The nodules in the kidney and liver were also recorded.

**Reverse transcription and quantitative real-time PCR.** Total RNA was extracted by Trizol (Life Technologies, Gaithersburg, MD) according to the manufacturer's instruction. One microgram RNA was subjected to reverse transcription using SuperScript III (Invitrogen, Carlsbad, CA). Real-time PCR was done with SYBR Green PCR Master Mix (Bio-Rad, Hercules, CA) at  $95^{\circ}\text{C}$  for 3 min and 40 cycles at  $95^{\circ}\text{C}$  for 30 s,  $58^{\circ}\text{C}$  for 30 s, and  $72^{\circ}\text{C}$  for 30 s on an iCycler iQ Multicolor Real-time PCR system (Bio-Rad). All samples were run in triplicate and data were analyzed using an iCycler iQ software (Bio-Rad). Primers used in real-time PCR were as follows: IGFBP-3, 5'-CGCCAGCTCCAGGAAATG-3' (forward) and 5'-GCATGCCCTTCTTGATGATG-3' (reverse); IGFBP-4, 5'-CCTCTACTTCATCCCATCC-3' (forward) and 5'-TCCACACACCAGCACITG-3' (reverse); IGFBP-5, 5'-TTGTCCACGCACCAGCAG-3' (forward) and 5'-AAAGCCAGCCCACGCATG-3' (reverse); and  $\beta$ -actin, 5'-TGTGCCCATCTACGAGGGGTATGC-3' (forward) and 5'-GGTACATGGTGTCGCCGCAGACA-3' (reverse).

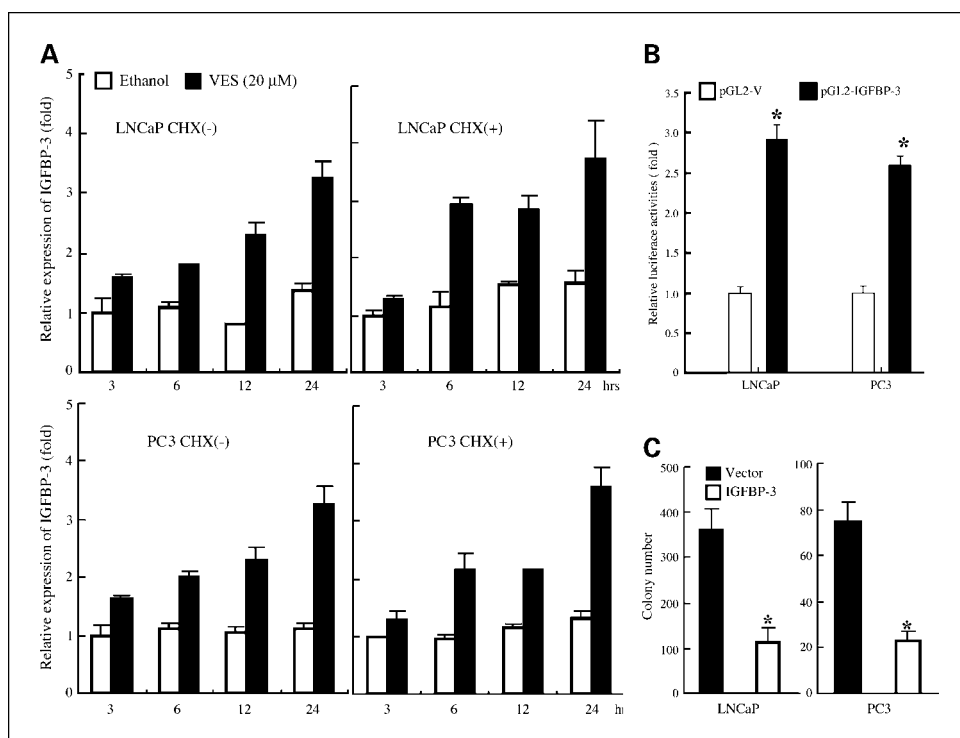
**Transfections and luciferase assay.** Cells were plated in 12-well plates. At 70% confluency, they were transfected for 24 h with 1  $\mu\text{g}$  DNA/well of vector or IGFBP-3 promoter-reporter construct (Dr. Youngman Oh, Virginia Commonwealth University Health System, Richmond VA) and 2 ng of the pRL-TK internal control using the Superfect reagent (Qiagen, Chatsworth, CA) followed by treatment with or without VES (20  $\mu\text{mol/L}$ ) in SFM for 18 h. Luciferase activities were measured as described previously and normalized with pRL-TK internal control (5).

**Colony formation assay.** Cells ( $1 \times 10^5$ ) were seeded into six-well plates and transfected with either pcDNA3.1-IGFBP-3 (Dr. David R. Clemmons, University of North Carolina, Chapel Hill, NC) or pcDNA3.1 empty vector with Superfect reagent. Approximately 24 h later, medium was replaced with fresh medium containing G418 (400  $\mu\text{g/mL}$ ). Two weeks later, the cells were fixed with 2% formaldehyde in  $1 \times$  PBS for 15 min and stained with 0.1% crystal violet in  $1 \times$  PBS for 15 min to assess colony formation. Colonies containing  $>40$  cells were counted. The experiments were repeated thrice in triplicate.

**Histology and immunohistochemistry analysis.** Tissues were processed as described previously (23). Histologic evaluations of TRAMP dorsolateral prostate were conducted by assessing changes that are characteristics for TRAMP prostate histology (24).

**Preparation of tissue extracts, cell lysates, and conditioned medium for Western blotting analysis.** After 12 h of serum starvation, cells were treated with vehicle or VES (20  $\mu\text{mol/L}$ ) for 24 or 48 h in SFM. Proteins from conditioned medium were concentrated 20-fold using Amicon Ultra15 centrifugal filter devices (Millipore, Bedford, MA). Cell lysates were prepared as described previously (10). Frozen xenografts or dorsolateral prostate tissues were pooled and homogenized in radioimmunoprecipitation assay buffer at  $4^{\circ}\text{C}$  to prepare tissue lysates. Cell and tissue lysates were clarified by centrifugation (12,000 rpm for 15 min at  $4^{\circ}\text{C}$ ) and equal amounts of denatured proteins were electrophoresed on a 10% SDS-polyacrylamide gel and transferred to Immobilon membrane (Millipore). Membranes were incubated with primary antibodies followed by a horseradish peroxidase-conjugated secondary antibody. Immunoreactive bands were detected using the enhanced chemiluminescence system (Amersham Biosciences, Piscataway, NJ).

**Fig. 2.** VES directly enhances IGFBP-3 expression at transcriptional level. **A**, VES-induced IGFBP-3 expression is not dependent on *de novo* protein synthesis. Serum-starved LNCaP and PC3 cells were treated with either vehicle or VES in SFM for 3, 6, 12, and 24 h in the absence or presence of cycloheximide (CHX; 10  $\mu\text{g/L}$ ). IGFBP-3 mRNA expression levels were analyzed by real-time PCR. **B**, VES enhances IGFBP-3 promoter luciferase activity. Cells were plated in 12-well plates for 36 h. At 70% confluency, cells were transfected with 1  $\mu\text{g}$  DNA/well of empty vector (pGL2) or IGFBP-3 promoter-reporter (pGL2-IGFBP-3) and 2 ng pRL-TK control followed by the treatment with or without 20  $\mu\text{mol/L}$  VES in SFM for 18 h. Luciferase activities in cell lysates were measured. The data point from pGL2-transfected cells with vehicle treatment is set as 1. **C**, overexpression of IGFBP-3 inhibits the colony formation capacity of LNCaP and PC3 cells. Cells were transfected with either pcDNA3.1 vector or pcDNA3.1-IGFBP-3 plasmid and selected with G418 for 2 wks. Colonies with  $>40$  cells were counted. Each experiment was done in triplicate and the experiment was repeated thrice independently. Columns, mean; bars, SD. \*,  $P < 0.05$ , compared with vehicle-treated control, Student's *t* test.



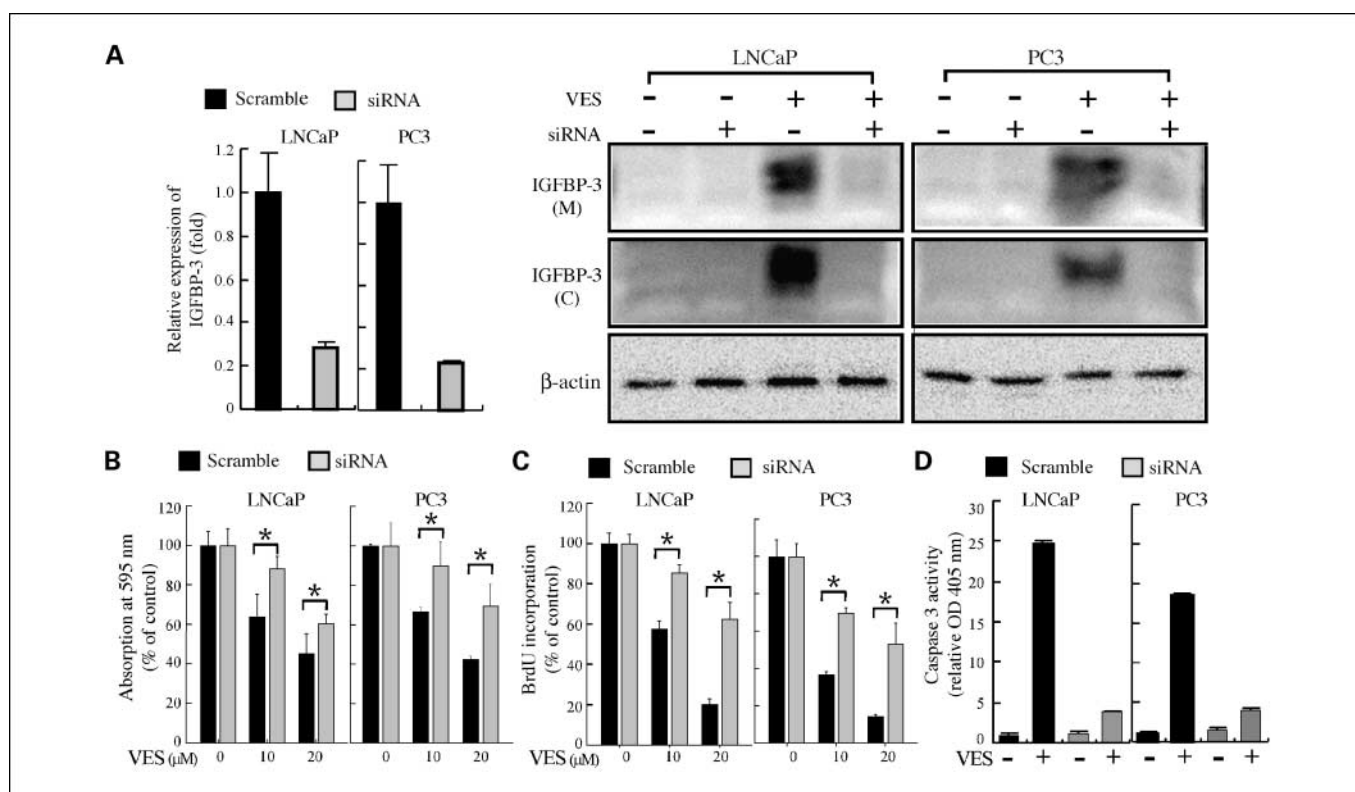


**Fig. 3.** Suppression of IGFBP-3 reduces the VES-mediated antiproliferative and proapoptotic effects. **A**, IGFBP-3 siRNA knocks down VES-induced IGFBP-3 protein expression. Cells were stably transfected with scramble or IGFBP-3 siRNA, cultured in SFM for 24 h, and then treated with either vehicle or 20  $\mu\text{mol/L}$  VES for additional 48 h. IGFBP-3 levels in concentrated conditioned medium and cytosol were examined by Western blotting analysis. **B**, suppression of IGFBP-3 reverses the VES-mediated growth inhibition. Cells were treated with either vehicle or VES in SFM. After 72 h, cell growth was monitored by 3-(4,5-dimethylthiazol-2-yl)-2,5-diphenyltetrazolium bromide assays. The results are reported as the relative absorption at 595 nm/L, considering control cells as 100%. **C**, knockdown of IGFBP-3 reverses VES-induced proliferation inhibition. Cells were treated with VES for 48 h and fixed, and DNA synthesis was assessed by bromodeoxyuridine (*BrdU*) colorimetric assay. The results are reported as the absorption at 450 nm/L, considering control cells as 100%. **D**, suppression of IGFBP-3 expression level diminishes the VES-mediated proapoptotic effect. Serum-starved cells were treated with 20  $\mu\text{mol/L}$  VES for 48 h. Caspase-3 activity was detected by colorimetric caspase-3 substrate I assay. The results are reported as the relative absorption at 405 nm/L, considering ethanol-treated control cells as 1. The experiments were repeated thrice with similar results. Columns, mean ( $n = 3$ ); bars, SD. \*,  $P < 0.05$ , compared with scramble control.

**Assessment of serum IGFBP-3 and IGF-I levels.** In athymic mouse serum, human IGFBP-3 secreted by LNCaP or PC3 cancer cells was determined by Quantikine human IGFBP-3 kit (R&D Systems, Minneapolis, MN). TRAMP mouse serum IGFBP-3 and IGF-I levels were determined by ELISA kits from Diagnostic Systems Laboratories.

**Apoptosis by ELISA assay.** Apoptosis was assessed as described previously (25) by Cell Death Detection ELISA Plus kit (Roche Molecular Biochemicals, Mannheim, Germany).

**3-(4,5-Dimethylthiazol-2-yl)-2,5-diphenyltetrazolium bromide assay.** Cells ( $1 \times 10^5$ - $2 \times 10^5$ ) were seeded in 12-well plates in 1 mL culture medium containing serum for 36 h. Cells were then washed with SFM and treated with 10 or 20  $\mu\text{mol/L}$  VES for 72 h. Cell growth was evaluated by 3-(4,5-dimethylthiazol-2-yl)-2,5-diphenyltetrazolium bromide assays as described previously (6).

**Proliferation assay by bromodeoxyuridine labeling.** Cells ( $2 \times 10^3$ - $5 \times 10^3$ ) were seeded in 100  $\mu\text{L}$  medium containing 10% serum per well in a 96-well plate for 36 h. Cells were then washed with SFM and treated with 10 or 20  $\mu\text{mol/L}$  VES for 48 h. The measurement was done following the manufacturer's protocol for the bromodeoxyuridine Labeling and Detection kit III (Roche, Mannheim, Germany).

**Caspase-3 activity measurement.** Caspase-3 activity was measured using the colorimetric caspase-3 substrate I (Calbiochem, La Jolla, CA). The absorbance values were measured at a wavelength of 405 nm on a plate reader (Molecular Devices, Inc., Sunnyvale, CA) at 15-min intervals for 2 h.

**Statistical analysis.** Genitourinary weights in TRAMP mice were compared among the groups using one-way ANOVA coupled with

Student-Newman-Keuls test. Other statistical analyses were done using the Student's *t* test. *P* values  $< 0.05$  were considered to be statistically significant.

## Results

**VES induces the expression of IGFBP-3 in human prostate cancer cells.** Serum-starved LNCaP and PC3 cells were treated with a series of increasing concentrations of VES in SFM. Real-time PCR results showed that VES induced IGFBP-3 mRNA in both cell lines in a dose-dependent manner (Fig. 1A). Consistently, the levels of IGFBP-3 protein in cell lysates and conditioned medium were stimulated by VES treatment in dose- and time-dependent manners in both prostate cancer cells (Fig. 1B). Intracellular and secreted IGFBP-3 protein levels were negligible or very low in untreated LNCaP and PC3 cells. Treatment with VES (10 and 20  $\mu\text{mol/L}$ ) for 24 and 48 h markedly induced IGFBP-3 expression. To test if VES selectively regulates the IGFBP-3 expression, we determine whether VES treatment can affect the expression of other members of IGFBP family. Indeed, our data showed that treatment with 20  $\mu\text{mol/L}$  VES for 24 h was unable to change mRNA expression of other high affinity IGFBP family members, including IGFBP-4 and IGFBP-5 in LNCaP and PC3 cells (Fig. 1C).



To determine whether the VES-induced IGFBP-3 levels is a primary response or secondary response requiring *de novo* protein synthesis, LNCaP and PC3 cells were treated with 10  $\mu\text{g}/\text{mL}$  cycloheximide for 30 min followed by cycloheximide plus 20  $\mu\text{mol}/\text{L}$  VES for 3, 6, 12, and 24 h. Real-time PCR results showed that the expression profiles of IGFBP-3 following VES treatment were not disturbed by cycloheximide treatment, indicating that new protein synthesis was not required for VES to exert its effect on IGFBP-3 mRNA expression (Fig. 2A). In addition, an IGFBP-3 promoter luciferase assay was used to confirm this primary response. In LNCaP and PC3 cells, VES (20  $\mu\text{mol}/\text{L}$ ) treatment increased the IGFBP-3 promoter activity by 2.9- and 2.6-fold, respectively (Fig. 2B).

To further explore the biological function of IGFBP-3 in prostate cancer cells, LNCaP and PC3 cells were transfected with IGFBP-3 expression plasmid (pcDNA3.1-IGFBP-3) or vector control following G418 selection for 2 weeks. As shown in Fig. 2C, overexpression of IGFBP-3 in LNCaP cells resulted in fewer colony numbers compared with the vector control

(113 versus 360). Similar results can be obtained from PC3 cells (23 versus 75). Together, our results indicate that VES directly enhances IGFBP-3 expression and higher expression of IGFBP-3 inhibits prostate cancer cell growth.

**IGFBP-3 is critical for VES to inhibit cell proliferation and induce apoptosis in prostate cancer cells.** To determine whether the VES-induced anticancer effects are dependent on IGFBP-3, we knocked down the IGFBP-3 expression using small interfering RNA (siRNA) strategy. Stable transfection of the IGFBP-3 siRNA was done as described previously (26). Results from real-time PCR indicated that IGFBP-3 mRNA expression was suppressed by  $\sim 70\%$ - $80\%$  in IGFBP-3 siRNA-transfected LNCaP and PC3 cells compared with scramble control (Fig. 3A), yet there was no effect on IGFBP-4 and IGFBP-5 mRNA levels (data not shown). The IGFBP-3 siRNA also inhibited VES-dependent induction of IGFBP-3 protein secreted into the conditioned medium or remained in the cytosol of LNCaP and PC3 cells (Fig. 3A).

To test whether the reduced IGFBP-3 expression could reverse the VES-mediated growth inhibition, IGFBP-3 siRNA

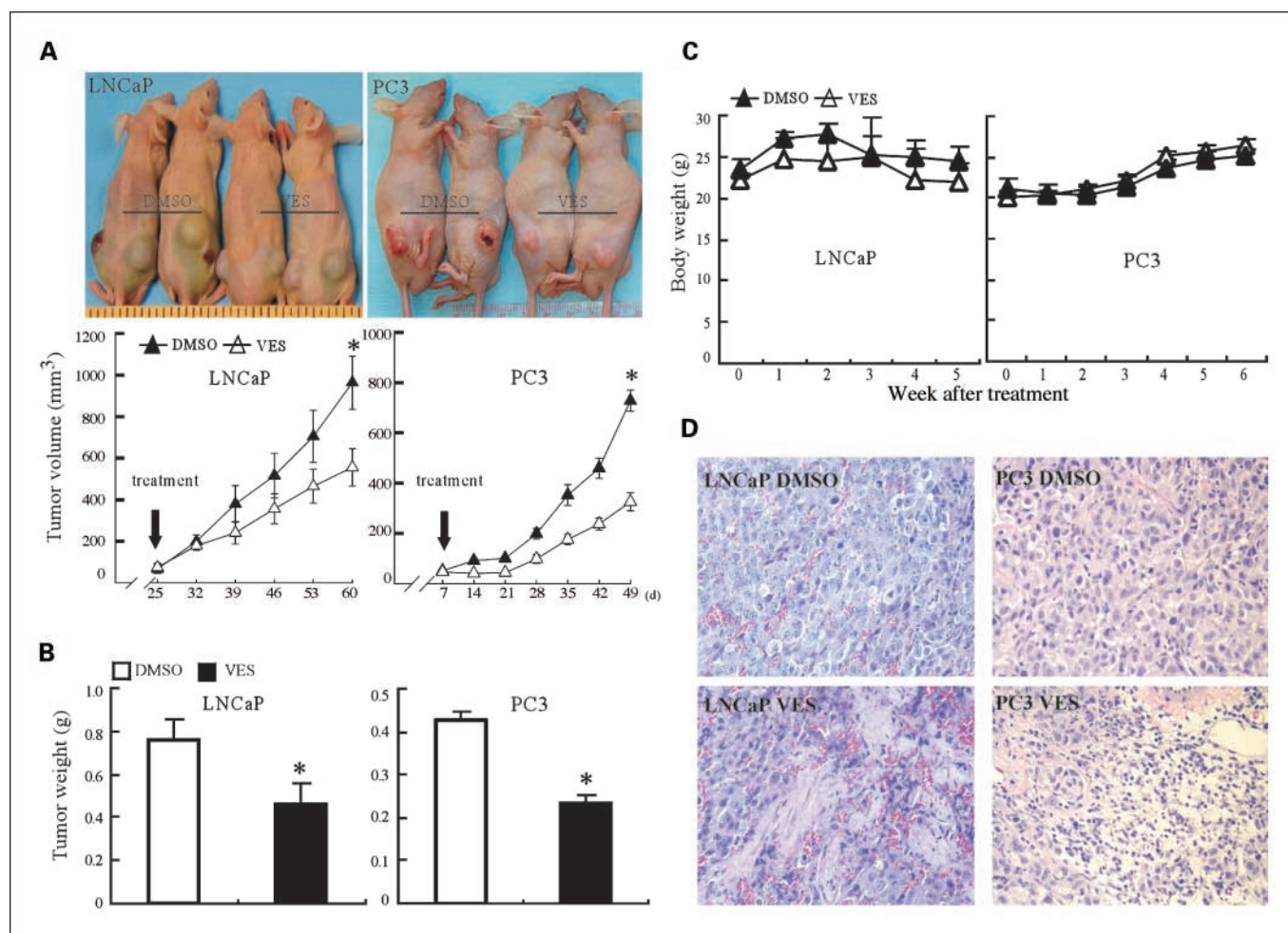


**Fig. 4.** Effects of VES on LNCaP and PC3 tumor xenografts in athymic male mice. **A**, tumor xenograft sizes are reduced by VES treatment. Tumor volume (mm<sup>3</sup>) was measured weekly throughout the study. Points, mean of 12 to 14 tumors in each group. **B**, xenograft tumor weights are reduced by VES treatment. Wet weights of the tumors were determined at autopsy. Columns, mean of 12 to 14 tumors from each group. **C**, body weight gain profiles of VES-treated and control nude mice. Body weight is represented as mean of seven mice in each group. **D**, histologic analyses of xenograft tumors in the presence or absence of VES treatment. LNCaP and PC3 control xenografts had poorly differentiated carcinoma cells without necrosis. Original magnification,  $\times 400$ . Xenografts from mice that received VES showed an increased proportion of noncellular stromal components and scattered necrotic lesions. \*,  $P < 0.05$ , compared with vehicle-treated control, Student's *t* test.

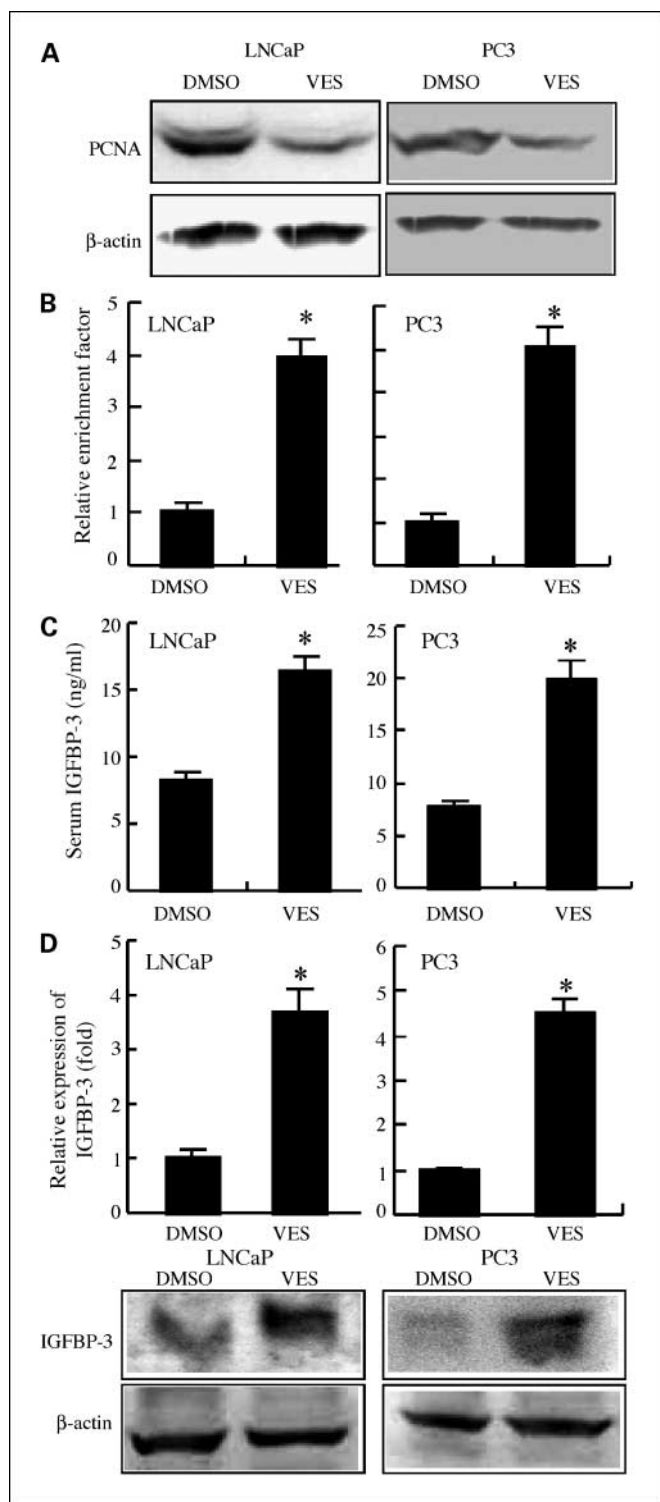


**Fig. 5.** Changes on molecular marker in VES-treated prostate tumor xenografts. **A**, VES treatment reduces the expression of PCNA. Sections of tumors were homogenized and protein extracts were immunoblotted with antibodies for PCNA and  $\beta$ -actin. **B**, VES treatment promotes apoptosis. Detection of apoptosis was done as per manufacturer's protocol. Data are expressed as relative enrichment factors, and result of vehicle-treated tumor is set as 1.0. **C**, VES treatment of nude mice induces the serum IGFBP-3 level produced by xenografted human prostate cancer tumors. Human IGFBP-3 concentrations in nude mice sera were assayed using ELISA kit ( $n = 7$ ). **D**, VES treatment enhances the mRNA and protein levels of IGFBP-3 in xenograft tumors. Data represent prostate lysate mixture from five mice in each group. \*,  $P < 0.05$ , compared with vehicle-treated TRAMP mice, Student's  $t$  test.

and scramble siRNA stably transfected cells were grown in either the presence or the absence of 10 or 20  $\mu\text{mol/L}$  VES for 72 h in SFM and their growth rates were evaluated (Fig. 3B). As expected, VES treatment resulted in a marked inhibition in cell proliferation in the scramble siRNA-transfected LNCaP and PC3 cells. In contrast, the response to VES, although not completely extinguished, was obviously reduced in IGFBP-3 siRNA-transfected LNCaP and PC3 cells. Similar results were also observed by the measurement of bromodeoxyuridine incorporation (Fig. 3C). These data indicate that VES-mediated growth inhibition is at least partly via IGFBP-3.

Because change of caspase-3 level was associated with both VES- and IGFBP-3-induced cell apoptosis pathways (27, 28), we further determined whether IGFBP-3 was involved in the VES-induced apoptosis by measuring caspase-3 activity. In scramble control LNCaP cells, although serum starvation alone resulted in basal levels of apoptosis, treatment of cells with VES resulted in a dramatic increase in caspase-3 activity, with a 25-fold increase over the basal level (Fig. 3D). In contrast, there is only 4-fold induction of caspase-3 activity in LNCaP-IGFBP-3 siRNA cells treated with 20  $\mu\text{mol/L}$  VES. Similar results were obtained in PC3 cells. Taken together, our siRNA knockdown data indicate that IGFBP-3 indeed mediates the VES-inhibited cell proliferation and VES-induced proapoptotic effect.

***I.p. administration of VES retards the growth of LNCaP and PC3 xenografts in vivo.*** To initiate the treatment on palpable size of tumor, LNCaP and PC3 xenograft were inoculated s.c. in nude mice. VES was then injected 25 days later for LNCaP and 7 days later for PC3 xenografts. VES administration significantly inhibited the growth of tumor xenografts compared with vehicle-treated controls. At sacrifice, the mean tumor volumes in animals treated with VES were  $556 \pm 89$  and  $325 \pm 35 \text{ mm}^3$  compared with  $963 \pm 127$  and  $728 \pm 42 \text{ mm}^3$  for control, in LNCaP and PC3 xenografts, respectively (Fig. 4A). The mean tumor weights in animals treated with VES were  $0.464 \pm 0.093$  and  $0.231 \pm 0.022 \text{ g}$  compared with  $0.764 \pm 0.095$  and  $0.425 \pm 0.021 \text{ g}$  for control, in LNCaP and PC3 xenografts, respectively (Fig. 4B). Notably, there was no overt gross toxicity in either group witnessed by measuring body weights (Fig. 4C) and histologic analyses of major organs, including brain, heart, lungs, liver, kidneys, spleen, spinal cord, gastrointestinal, and genitourinary tract (data not shown). Increased proportions of noncellular stroma components and scattered necrotic lesions were observed in the tumor from VES-treated mice (Fig. 4D).

***VES treatment suppresses cell proliferation and induces apoptosis in xenograft tumors of nude mice.*** To determine whether VES-mediated tumor inhibition was due to low proliferation rates and/or apoptosis induction, we examined the proliferation of xenograft tumors by assessing PCNA expression and apoptosis by assessing the amount of cleared DNA/histone complexes. VES treatment resulted in a significant reduction in PCNA protein expression and marked induction of apoptosis in LNCaP and PC3 xenograft tumors compared with the vehicle control (Fig. 5A and B).

***VES treatment increases IGFBP-3 levels in nude mice.*** The effects of VES treatment on serum levels of human IGFBP-3 produced by human prostate cancer LNCaP and PC3 xenografts were determined by ELISA (Fig. 5C). Our results yielded  $16.29 \pm 1.28$  and  $19.75 \pm 1.92 \text{ ng/mL}$  human IGFBP-3 in serum of VES-treated mice compared with  $7.71 \pm 0.65$  and

8.18 ± 0.79 ng/mL for control mice, in LNCaP and PC3 xenografts, respectively. VES treatment resulted in smaller prostate tumor mass with increased human IGFBP-3 in nude mouse serum. Consistent with the changes in serum level, increases of the IGFBP-3 mRNA and protein expression levels were also observed in VES-treated LNCaP and PC3 xenografts compared with the vehicle control (Fig. 5D).

**VES treatment prevents prostate cancer progression in TRAMP mice.** We further showed the preventive efficacy of VES in TRAMP mouse model, which is an excellent preclinical model for study of the chemopreventive effect of compounds on prostate cancer (17, 22). By 28 to 32 weeks, the typical prostate phenotype of C57BL/6 genetic background TRAMP mouse exhibits prostate tumor with infiltrated seminal vesicles (29). The wet weights of the genitourinary tract have been used to evaluate the prevention efficacy of various compounds (29). At the age of 32 weeks, VES treatments decreased the size and weight of genitourinary tract with tumors in a dose-dependent manner compared with age-matched vehicle-treated TRAMP mice (Fig. 6A). The average genitourinary tract weights of vehicle-treated and VES-treated (50 and 100 mg/kg) TRAMP mice were 2.71 ± 0.28, 1.42 ± 0.15, and 0.80 ± 0.05 g, respectively. That of age-matched nontransgene littermates was 0.47 ± 0.06 g (Fig. 6A).

To examine whether VES treatment affects the expression level of SV40 large T-ag, Western blot analysis was applied on prostate tissue extracts from TRAMP mice treated with or without 100 mg/kg VES for 8 weeks. There was no significant change of the T-ag expression level in prostate tumor tissue obtained from TRAMP mice treated with or without VES (Fig. 6A). Additionally, the effect of VES on T-ag was determined in the prostates of 32-week-old TRAMP mice by immunohistochemistry staining and was found to be detectable in both VES and DMSO groups (data not shown). Therefore, VES preventive effect was not due to a change in the expression of the T-ag.

There was no significant change of body weight among different treatments, although vehicle-treated TRAMP mice had a slightly larger body weight compared with the VES treatment group (Fig. 6A). This might be due to the enlarged genitourinary tract with larger tumor mass. We also evaluated the toxicity of VES in the nontransgene littermates. The mean body weights and histologic analyses of several organs from VES-treated mice did not show any appreciable changes (data not shown).

The antitumor ability of VES was further investigated by histologic analysis. We found that the dorsolateral prostate of the age-matched nontransgene male littermates had delicate epithelial ducts with sparse intervening stroma at 32 weeks of age. In contrast, histologic examination of a typical vehicle-treated TRAMP prostate sample at 32 weeks of age revealed well to poorly differentiated prostate cancer with sheets of malignant cells and with little or no gland-like structure. Conversely, the experimental group of 50 and 100 mg/kg VES-treated mice exhibited well-differentiated and PIN-type lesions (Fig. 6B). There was no poorly differentiated stage found in the mice treated with VES at either of the VES doses.

The cumulative data at the termination of the experiment (32 weeks of age) from 12 animals in the vehicle-treated group showed 100% invasive tumors, which metastasized to lymph node (12 of 12), lung (4 of 12), liver (4 of 12), and kidney (3

of 12). In contrast, with two doses of VES treatment, none of the 24 mice exhibited metastases to liver and kidney, only 3 of 24 developed lymph metastases, and 1 of 24 developed lung metastases (Fig. 6B).

**Inhibition of TRAMP mouse prostate cancer progression by VES treatment is associated with the increase in apoptosis and decrease in proliferation.** TRAMP mouse dorsolateral prostate lysates from each of the treatments were examined for PCNA protein levels by Western blotting analysis. As shown in Fig. 6C (top), VES treatment reduced the PCNA protein expression in TRAMP prostate lysates.

Furthermore, results from ELISA assay indicated that i.p. administration of VES resulted in marked dose-dependent induction of apoptosis in dorsolateral prostate tissues of TRAMP mice (Fig. 6C, bottom).

**VES treatment increases the IGFBP-3 level without altering the IGF-I level in the TRAMP mouse prostate cancer model.** We further determined the levels of IGFBP-3 in the serum and prostate tissues of VES-treated and control TRAMP mice. Consistent with previous findings, vehicle-treated TRAMP mice maintained lower serum IGFBP-3 at the age of 32 weeks compared with the nontransgenic littermates. However, 50 and 100 mg/kg VES treatments increased the serum IGFBP-3 levels (Fig. 6D). The serum IGFBP-3 levels in the vehicle-treated TRAMP, the 50 and 100 mg/kg VES-treated TRAMP mice, and the age-matched nontransgene male littermates were 7.38 ± 0.05, 8.61 ± 0.28, 11.19 ± 0.59, and 14.85 ± 0.15 ng/mL, respectively (Fig. 6D). Because IGFBP-3 levels might be regulated by growth factor IGF-I and most studies indicate that prostate epithelial cells, such as LNCaP, DU145 (30), and PC3 (31), are not able to produce IGF-I or only a small amount that is insufficient to stimulate growth, we detected the serum level of IGF-I in TRAMP mice. Notably, VES treatment had no significant effect on serum level of IGF-I (Fig. 5D). Consistently, mRNA and protein levels of IGFBP-3 in the dorsolateral prostate had a similar changing pattern as serum IGFBP-3 (Fig. 6D).

Collectively, our data indicate that antiproliferation and proapoptosis were involved in the preventive and therapeutic effects of VES, which were associated with induction of IGFBP-3 in both tissue and serum levels.

## Discussion

VES has drawn significant attention due to its potent anticancer activities. Although there is a growing body of evidence supporting the existence of multiple mechanisms for its biological activities (3, 5, 6, 8, 9), details about these mechanisms and the molecular targets of VES remain largely unknown. In this study, we show that VES up-regulates the expression of IGFBP-3 in prostate cancer cells and preclinical prostate cancer animal models. This VES-enhanced IGFBP-3, consequently inhibiting the proliferation and inducing apoptosis of cancer cells, could be one of the possible mechanisms that accounts for the therapeutic and preventive efficacy of VES in prostate cancer.

The IGFBP-3 protein has emerged as one of the critical regulators in modulating cell proliferation and apoptosis (19). A higher IGFBP-3 serum level is associated with a lower incidence of cancer (14). The functional mechanisms of IGFBP-3 include IGF-dependent and IGF-independent action (32).



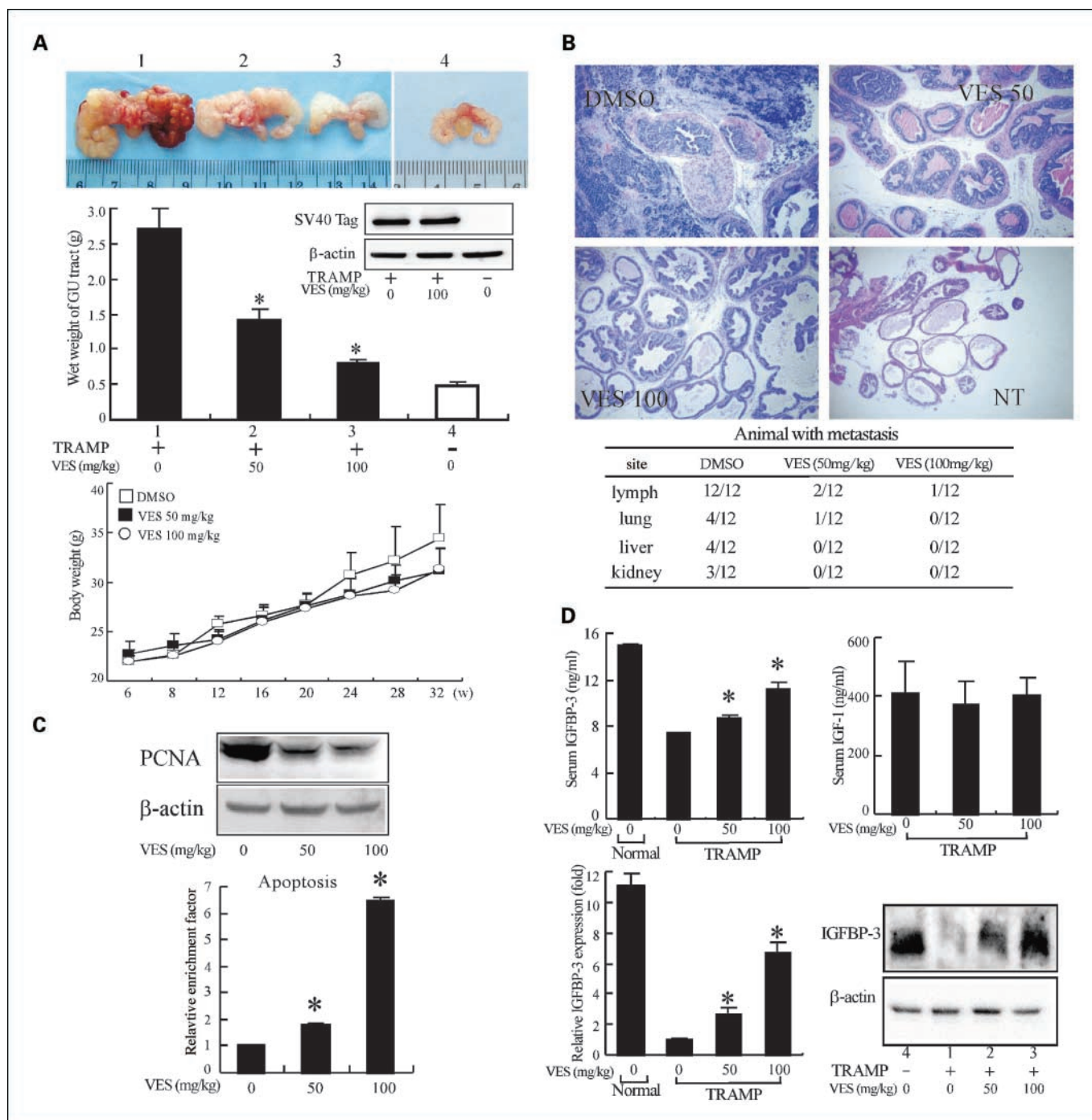


**Fig. 6.** VES inhibits prostate cancer progression in TRAMP mice. **A**, VES treatment reduces the mass of prostate cancer tissues invading to genitourinary area without overt toxicity in TRAMP mice. The lower genitourinary tracts were dissected and weighed from age-matched TRAMP mice (1, vehicle; 2, 50 mg/kg VES; 3, 100 mg/kg VES) and nontransgene littermates (4, vehicle). The weight gain profiles of TRAMP (vehicle, 50 mg/kg VES, and 100 mg/kg VES) from 6 to 32 wks. SV40 T-ag protein has no significant change in the presence or absence of VES treatment for 8 wks. Columns, wet weight of genitourinary (GU) tract (10-12 mice); points, body weight (10-12 mice); bars, SE. **B**, effect of VES on histologic features of prostate and metastasis in TRAMP mice. **C**, VES inhibits the PCNA protein level and induces apoptosis in TRAMP prostate tumor. Protein extracts from pooled dorsolateral prostates were immunoblotted with PCNA antibody. Apoptosis assay was done following the manufacturer's protocol, and data are expressed as enrichment factor. **D**, VES treatment increases the IGFBP-3 levels without alteration of IGF-1 levels in TRAMP mice. Blood was withdrawn at autopsy and serum IGFBP-3 and IGF-1 levels were analyzed by ELISA. IGFBP-3 mRNA and protein levels were examined from the pooled dorsolateral prostates of 32-week-old TRAMP mice and age-matched nontransgene littermates and evaluated by real-time PCR and Western blotting analyses. Data represent prostate lysate mixture from five animals in each group. \*,  $P < 0.05$ , compared with vehicle-treated TRAMP mice.

IGFBP-3 is a critical requirement for apoptosis induced by multiple stimuli in human cancer cells (32). Furthermore, IGFBP-3 alone or in combination with chemotherapeutic agents exhibits potent antitumor activity *in vitro* and *in vivo*

(33). Moreover, anticancer effects of several dietary factors, including silibinin (34), green tea (35), grape seed extract (36), and apigenin (37), are associated with elevated IGFBP-3 levels. In addition, some of the most potent antiproliferative factors,



such as tumor necrosis factor- $\alpha$  (38), transforming growth factor- $\beta$  (39), retinoic acid (40), p53 (41), and vitamin D<sub>3</sub> (35), function at least partially via induction of IGFBP-3 expression. All these studies indicate that IGFBP-3 is possibly one important molecular target for antitumor therapy.

We showed that VES induced both mRNA and protein expressions of IGFBP-3 in prostate cancer cells in time- and dose-dependent manners. The mechanism is at least partially through enhanced IGFBP-3 promoter activity. To further assess the role of elevated IGFBP-3 in the VES-mediated antiproliferative and proapoptotic effects, we used the specific IGFBP-3 siRNA to knock down the expression of IGFBP-3 and examined whether the forced reduction of IGFBP-3 could block the VES-mediated antiproliferative and proapoptotic effects. Indeed, the specific knockdown of IGFBP-3 dramatically diminished the VES-mediated antiproliferative effect. Our results suggest that the promoter of IGFBP-3 could have a potential VES response element. Although VES can regulate several molecular pathways to achieve its anticancer effects, there is still no demonstrated promoter response element specifically responding to VES treatment. Further studies are required to clarify the mechanisms by which VES enhances the expression of IGFBP-3.

Accumulating evidences indicate that  $\alpha$ -vitamin E not only suppresses proliferation of cancer cells in culture but also offers protection against carcinogen-induced cancer in animal models. Studies have indicated that VES has inhibitory effects on the proliferation of cultured prostate cancer cells that could be due to cell cycle interruption as well as apoptosis induction (3, 6). Although oral intake of VES, selenium, and lycopene mixtures showed preventive effects on prostate cancer development in the LADY model (42), it is argued that this preventive effect is not contributed by VES alone, and it is also argued whether VES retains its intact structure after oral intake. The present study provides clear experimental evidence to indicate that VES is capable of exerting therapeutic and preventive effects on prostate cancer development without notable toxicity in TRAMP mice after i.p. administration of VES. VES is an ester derivative of the naturally occurring RRR form of  $\alpha$ -vitamin E. Its basic structure has the potential to compromise its potency via oral administration [i.e., the ester linkage can be hydrolyzed by cellular esterases, yielding  $\alpha$ -vitamin E (RRR- $\alpha$ -tocopherol) and succinic acid, neither of

which exhibits effective anticancer properties; ref. 5]. The ineffectiveness of oral VES delivery was expected based on *in vitro* analyses showing that antitumor activities required the intact compound and the potential for deesterification by intestinal esterases (43, 44). Although VES has been proven to be a potent anticancer agent both *in vitro* and *in vivo*, its basic structure limits its wide application. Therefore, synthesis of more stable VES analogues is needed in the near future.

Prevention is a relatively new and promising strategy that uses natural or synthetic agents to delay, halt, or even reverse the process of carcinogenesis (45). Prostate cancer is a good chemopreventive candidate because of its high incidence and long latency between the initiation of the premalignant latent phase and progression to invasive prostate cancer (46). Prevention of prostate cancer should be a primary research goal, but human studies of nutrition and dietary agents are limited by the long latency periods and challenging epidemiologic considerations. The TRAMP model, which affects several molecular pathways for developing multistage prostate tumorigenesis, is a well-studied autochthonous transgenic animal model of prostate cancer (21). In addition, male TRAMP mice could develop progressive prostate cancer that mimics human disease with metastatic spread to distant sites. This model has been used to evaluate the prevention efficiency of several agents against prostate cancer (17, 22, 47–49). The ideal preventive agent will either inhibit or slow tumor growth with a low level of toxicity or side effects. VES-treated mice maintained their body weight and physical activity, suggesting that the effective dose of VES, which suppresses tumor progression, is well tolerated and nontoxic.

Taken together, we have shown that VES stimulated the expression of IGFBP-3 *in vitro* and *in vivo*, which contributed to prostate cancer therapeutic and preventive effects mediated by VES. Knockdown of IGFBP-3 by siRNA strategy effectively diminished VES-mediated antiproliferative and proapoptotic function. We provide solid evidences that IGFBP-3 is critical for VES-mediated antitumor functions.

## Acknowledgments

We thank Dr. Raymond B. Baggs for histologic analysis, Dr. Chawnsiang Chang for helpful discussions, Karen Wolf for manuscript preparation, Dr. Youngman Oh for providing pGL2-IGFBP-3 plasmid, Dr. Hiroshi Nakagawa for the IGFBP-3 siRNA, and Dr. David R. Clemmons for the pCDNA3-IGFBP-3 plasmid.

## References

- Jemal A, Siegel R, Ward E, et al. Cancer statistics, 2006. *CA Cancer J Clin* 2006;56:106–30.
- Sung L, Greenberg ML, Koren G, et al. Vitamin E: the evidence for multiple roles in cancer. *Nutr Cancer* 2003;46:1–14.
- Israel K, Yu W, Sanders BG, Kline K. Vitamin E succinate induces apoptosis in human prostate cancer cells: role for Fas in vitamin E succinate-triggered apoptosis. *Nutr Cancer* 2000;36:90–100.
- Yu W, Israel K, Liao QY, et al. Vitamin E succinate (VES) induces Fas sensitivity in human breast cancer cells: role for M<sub>r</sub> 43,000 Fas in VES-triggered apoptosis. *Cancer Res* 1999;59:953–61.
- Zhang Y, Ni J, Messing EM, et al. Vitamin E succinate inhibits the function of androgen receptor and the expression of prostate-specific antigen in prostate cancer cells. *Proc Natl Acad Sci U S A* 2002;99:7408–13.
- Ni J, Chen M, Zhang Y, et al. Vitamin E succinate inhibits human prostate cancer cell growth via modulating cell cycle regulatory machinery. *Biochem Biophys Res Commun* 2003;300:357–63.
- Venkateswaran V, Fleshner NE, Klotz LH. Modulation of cell proliferation and cell cycle regulators by vitamin E in human prostate carcinoma cell lines. *J Urol* 2002;168:1578–82.
- Israel K, Sanders BG, Kline K. RRR- $\alpha$ -tocopheryl succinate inhibits the proliferation of human prostatic tumor cells with defective cell cycle/differentiation pathways. *Nutr Cancer* 1995;24:161–9.
- Zhang M, Altuwaijri S, Yeh S. RRR- $\alpha$ -tocopheryl succinate inhibits human prostate cancer cell invasiveness. *Oncogene* 2004;23:3080–8.
- Ni J, Wen X, Yao J, et al. Tocopherol-associated protein suppresses prostate cancer cell growth by inhibition of the phosphoinositide 3-kinase pathway. *Cancer Res* 2005;65:9807–16.
- Ni J, Pang S, Yeh S. Different retention of  $\alpha$ -vitamin E is correlated with its transporter gene expression and growth inhibition efficacy in prostate cancer cells. *Prostate*. Epub 2007; Jan 24.
- Chan JM, Stampfer MJ, Giovannucci E, et al. Plasma insulin-like growth factor-I and prostate cancer risk: a prospective study. *Science* 1998;279:563–6.
- Chan JM, Stampfer MJ, Ma J, et al. Insulin-like growth factor-I (IGF-I) and IGF binding protein-3 as predictors of advanced-stage prostate cancer. *J Natl Cancer Inst* 2002;94:1099–106.
- Chen C, Lewis SK, Voigt L, et al. Prostate carcinoma incidence in relation to prediagnostic circulating levels of insulin-like growth factor I, insulin-like growth factor binding protein 3, and insulin. *Cancer* 2005;103:76–84.
- Palmqvist R, Hallmans G, Rinaldi S, et al. Plasma insulin-like growth factor 1, insulin-like growth factor binding protein 3, and risk of colorectal cancer: a prospective study in northern Sweden. *Gut* 2002;50:642–6.

16. Wakai K, Ito Y, Suzuki K, et al. Serum insulin-like growth factors, insulin-like growth factor-binding protein-3, and risk of lung cancer death: a case-control study nested in the Japan Collaborative Cohort (JACC) Study. *Jpn J Cancer Res* 2002;93:1279–86.
17. Gupta S, Hastak K, Ahmad N, Lewin JS, Mukhtar H. Inhibition of prostate carcinogenesis in TRAMP mice by oral infusion of green tea polyphenols. *Proc Natl Acad Sci U S A* 2001;98:10350–5.
18. Firth SM, Baxter RC. Cellular actions of the insulin-like growth factor binding proteins. *Endocr Rev* 2002;23:824–54.
19. Ali O, Cohen P, Lee KW. Epidemiology and biology of insulin-like growth factor binding protein-3 (IGFBP-3) as an anti-cancer molecule. *Horm Metab Res* 2003;35:726–33.
20. Silha JV, Sheppard PC, Mishra S, et al. Insulin-like growth factor (IGF) binding protein-3 attenuates prostate tumor growth by IGF-dependent and IGF-independent mechanisms. *Endocrinology* 2006;147:2112–21.
21. Greenberg NM, DeMayo F, Finegold MJ, et al. Prostate cancer in a transgenic mouse. *Proc Natl Acad Sci U S A* 1995;92:3439–43.
22. Gupta S, Ahmad N, Marengo SR, et al. Chemoprevention of prostate carcinogenesis by  $\alpha$ -difluoromethylornithine in TRAMP mice. *Cancer Res* 2000;60:5125–33.
23. Yeh S, Hu YC, Wang PH, et al. Abnormal mammary gland development and growth retardation in female mice and MCF7 breast cancer cells lacking androgen receptor. *J Exp Med* 2003;198:1899–908.
24. Shappell SB, Thomas GV, Roberts RL, et al. Prostate pathology of genetically engineered mice: definitions and classification. The consensus report from the Bar Harbor meeting of the Mouse Models of Human Cancer Consortium Prostate Pathology Committee. *Cancer Res* 2004;64:2270–305.
25. Gupta S, Adhami VM, Subbarayan M, et al. Suppression of prostate carcinogenesis by dietary supplementation of celecoxib in transgenic adenocarcinoma of the mouse prostate model. *Cancer Res* 2004;64:3334–43.
26. Takaoka M, Harada H, Andl CD, et al. Epidermal growth factor receptor regulates aberrant expression of insulin-like growth factor-binding protein 3. *Cancer Res* 2004;64:7711–23.
27. Lee HY, Chun KH, Liu B, et al. Insulin-like growth factor binding protein-3 inhibits the growth of non-small cell lung cancer. *Cancer Res* 2002;62:3530–7.
28. Yu W, Sanders BG, Kline K. RRR- $\alpha$ -tocopheryl succinate-induced apoptosis of human breast cancer cells involves Bax translocation to mitochondria. *Cancer Res* 2003;63:2483–91.
29. Kaplan-Lefko PJ, Chen TM, Ittmann MM, et al. Pathobiology of autochthonous prostate cancer in a pre-clinical transgenic mouse model. *Prostate* 2003;55:219–37.
30. Kawada M, Inoue H, Masuda T, Ikeda D. Insulin-like growth factor I secreted from prostate stromal cells mediates tumor-stromal cell interactions of prostate cancer. *Cancer Res* 2006;66:4419–25.
31. Kaicer EK, Blat C, Harel L. IGF-I and IGF-binding proteins: stimulatory and inhibitory factors secreted by human prostatic adenocarcinoma cells. *Growth Factors* 1991;4:231–7.
32. Renehan AG, Zwahlen M, Minder C, et al. Insulin-like growth factor (IGF)-I, IGF binding protein-3, and cancer risk: systematic review and meta-regression analysis. *Lancet* 2004;363:1346–53.
33. Liu B, Lee KW, Li H, et al. Combination therapy of insulin-like growth factor binding protein-3 and retinoid X receptor ligands synergize on prostate cancer cell apoptosis *in vitro* and *in vivo*. *Clin Cancer Res* 2005;11:4851–6.
34. Singh RP, Dhanalakshmi S, Tyagi AK, et al. Dietary feeding of silibinin inhibits advanced human prostate carcinoma growth in athymic nude mice and increases plasma insulin-like growth factor-binding protein-3 levels. *Cancer Res* 2002;62:3063–9.
35. Boyle BJ, Zhao XY, Cohen P, Feldman D. Insulin-like growth factor binding protein-3 mediates 1  $\alpha$ ,25-dihydroxyvitamin d(3) growth inhibition in the LNCaP prostate cancer cell line through p21/WAF1. *J Urol* 2001;165:1319–24.
36. Singh RP, Tyagi AK, Dhanalakshmi S, Agarwal R, Agarwal C. Grape seed extract inhibits advanced human prostate tumor growth and angiogenesis and upregulates insulin-like growth factor binding protein-3. *Int J Cancer* 2004;108:733–40.
37. Shukla S, Mishra A, Fu P, et al. Up-regulation of insulin-like growth factor binding protein-3 by apigenin leads to growth inhibition and apoptosis of 22Rv1 xenograft in athymic nude mice. *FASEB J* 2005;19:2042–4.
38. Rajah R, Lee KW, Cohen P. Insulin-like growth factor binding protein-3 mediates tumor necrosis factor- $\alpha$ -induced apoptosis: role of Bcl-2 phosphorylation. *Cell Growth Differ* 2002;13:163–71.
39. Hwa V, Oh Y, Rosenfeld RG. Insulin-like growth factor binding protein-3 and -5 are regulated by transforming growth factor- $\beta$  and retinoic acid in the human prostate adenocarcinoma cell line PC-3. *Endocrine* 1997;6:235–42.
40. Gucev ZS, Oh Y, Kelley KM, Rosenfeld RG. Insulin-like growth factor binding protein 3 mediates retinoic acid- and transforming growth factor  $\beta$ 2-induced growth inhibition in human breast cancer cells. *Cancer Res* 1996;56:1545–50.
41. Grimberg A, Liu B, Bannerman P, El-Deiry WS, Cohen P. IGFBP-3 mediates p53-induced apoptosis during serum starvation. *Int J Oncol* 2002;21:327–35.
42. Venkateswaran V, Fleschner NE, Sugar LM, Klotz LH. Antioxidants block prostate cancer in lady transgenic mice. *Cancer Res* 2004;64:5891–6.
43. Andreasen MF, Kroon PA, Williamson G, Garcia-Conesa MT. Intestinal release and uptake of phenolic antioxidant diferulic acids. *Free Radic Biol Med* 2001;31:304–14.
44. Andreasen MF, Kroon PA, Williamson G, Garcia-Conesa MT. Esterase activity able to hydrolyze dietary antioxidant hydroxycinnamates is distributed along the intestine of mammals. *J Agric Food Chem* 2001;49:5679–84.
45. Gupta S. Prostate cancer chemoprevention: models, limitations, and potential [review]. *Int J Oncol* 2004;25:1133–48.
46. Kelloff GJ, Lieberman R, Brawer MK, et al. Strategies for chemoprevention of prostate cancer. *Prostate Cancer Prostatic Dis* 1999;2:27–33.
47. Mentor-Marcel R, Lamartiniere CA, Eltoum IE, Greenberg NM, Elgavish A. Genistein in the diet reduces the incidence of poorly differentiated prostatic adenocarcinoma in transgenic mice (TRAMP). *Cancer Res* 2001;61:6777–82.
48. Raghov S, Hooshdaran MZ, Katiyar S, Steiner MS. Toremifene prevents prostate cancer in the transgenic adenocarcinoma of mouse prostate model. *Cancer Res* 2002;62:1370–6.
49. Raghov S, Kuliye E, Steakley M, Greenberg N, Steiner MS. Efficacious chemoprevention of primary prostate cancer by flutamide in an autochthonous transgenic model. *Cancer Res* 2000;60:4093–7.